Technical University of Denmark

DTU

Experimental and kinetic modeling study of C2H4 oxidation at high pressure

Lopez, Jorge Gimenez; Rasmussen, Christian Lund; Alzueta, Maria; Gao, Yide; Marshall, Paul; Glarborg, Peter

DTU Library
Technical Information Center of Denmark

Experimental and Kinetic Modeling Study of C_2H_4 Oxidation at High Pressure

Jorge Gimenez Lopez[1,2], Christian Lund Rasmussen[1], Maria U. Alzueta[2], Yide Gao[3], Paul Marshall[3], and Peter Glarborg[1]

[1] *Department of Chemical and Biochemical Engineering, Technical University of Denmark, DK-2800 Kgs. Lyngby, Denmark*

[2] *Department of Chemical and Environmental Engineering, University of Zaragoza, 50018 Zaragoza, Spain*

[3] *Department of Chemistry, University of North Texas, Denton, Texas 76203-5070*

A detailed chemical kinetic model for oxidation of C_2H_4 in the intermediate temperature range and high pressure has been developed and validated experimentally. New ab initio calculations and RRKM analysis of the important $C_2H_3 + O_2$ reaction was was used to obtain rate coefficients over a wide range of conditions (0.003-100 bar, 200–3000 K). The results indicate that at 60 bar vinyl peroxide, rather than CH_2O and HCO, is the dominant product. The experiments, involving C_2H_4/O_2 mixtures diluted in N_2, were carried out in a high pressure flow reactor at 600–900 K and 60 bar, varying the reaction stoichiometry from very lean to fuel-rich conditions. Model predictions are generally satisfactory. The governing reaction mechanisms are outlined based on calculations with the kinetic model. Under the investigated conditions the oxidation pathways for C_2H_4 are more complex than those prevailing at higher temperatures and lower pressures. The major differences are the importance of the hydroxyethyl (CH_2CH_2OH) and 2-hydroperoxyethyl

(CH$_2$CH$_2$OOH) radicals, formed from addition of OH and HO$_2$ to C$_2$H$_4$, and vinyl peroxide, formed from C$_2$H$_3$ + O$_2$. Hydroxyethyl is oxidized through the peroxide HOCH$_2$CH$_2$OO (lean conditions) or through ethenol (low O$_2$ concentration), while 2-hydroperoxyethyl is converted through oxirane.

Introduction

Ethylene (C_2H_4) is an important intermediate in combustion of hydrocarbons as well as in atmospheric chemistry. Previous studies of C_2H_4 oxidation have been conducted in static reactors [1], flow reactors [2–7], shock tubes [8–12] and premixed laminar flames [13–17], covering a wide range of stoichiometries and temperatures. Most of the reported work, however, have been carried out at near atmospheric pressure. A few results are available from flow reactor studies at 5-10 bar [6], but despite their relevance for the chemistry in engines, gas turbines, and gas-to-liquid processes, data at high pressures are limited.

The objective of the present study is to obtain experimental results for the oxidation of C_2H_4 at high pressure (60 bar) as functions of temperature (600–900 K) and stoichiometry (lean to fuel-rich) and analyze them in terms of a detailed chemical kinetic model. The oxidation pathways for C_2H_4 under these conditions are different from those prevailing at higher temperatures and lower pressures and the results of the current work help to extend the validation range for chemical kinetic modeling of C_2H_4 oxidation. This paper is part of a series investigating the high-pressure, medium temperature oxidation of simple fuels: previously work has been reported for CO/H_2, CH_4, and CH_4/C_2H_6 mixtures [18, 19]. The present kinetic model draws on this work, as well as recent results in tropospheric chemistry. Furthermore, the important reaction of C_2H_3 with O_2 was characterized from ab initio calculations over a wide range of pressure and temperature.

Experimental

The experimental setup is a laboratory-scale high pressure laminar flow reactor designed to approximate plug-flow. The setup is described in detail elsewhere [18] and only a brief description is provided here. The system enables well-defined investigations of homogeneous gas phase chemistry at pressures from 10 to 100 bar, temperatures up to 925 K, and flow rates of 1–5 L min^{-1} (STP). The reactions take place in a tubular quartz reactor, enclosed in a stainless steel tube that acts as a pressure shell. The steel tube is placed in a tube oven with three individually controlled electrical heating elements that produce an isothermal reaction zone (± 5 K) of 43 cm. The reactor temperature is monitored by type K thermo-couples (± 2.2 K or 0.75 %) positioned in the void between the quartz reactor and the steel shell.

The reactant gases are premixed before entering the reactor. All gases used in the experiments are high purity gases or mixtures with certified concentrations ($\pm 2\%$ uncertainty). The system is pressurized from the feed gas cylinders. Downstream of the reactor, the system pressure is reduced to atmospheric level prior to product analysis, which is conducted by an on-line 6890N Agilent Gas Chromatograph (GC-TCD/FID from Agilent Technologies). The GC allows detection of O_2, CO, CO_2, C_2H_6, C_2H_4, C_2H_2, and CH_4 with an overall relative measuring uncertainty in the range $\pm 6\%$.

Experimental data are obtained as mole fractions as a function of the reactor temperature measured at intervals of 25 K. The reactor operates in the laminar flow regime, but under conditions tailored to approximate plug flow [18].

Detailed Kinetic Model

The starting mechanism and corresponding thermodynamic properties were drawn from previous high-pressure work on oxidation of CO/H_2, CH_4, and CH_4/C_2H_6 [18, 19]. The only change in the C_1 subset was the omission of the reaction $HOCO+OH \rightleftharpoons CO+H_2O_2$, pending further investigation. In the present work the C_2H_4 oxidation subset of the mechanism was updated, with particular emphasis on a number of oxygenated C_2-species important under low-temperature conditions. The thermodynamic properties for some of these species are shown in Table 1, while Table 2 lists key reactions in the C_2H_4 oxidation scheme. The full mechanism is available as supplemental material. The low-to-medium temperature oxidation chemistry for ethylene at atmospheric pressure was previously discussed by Wilk et al. [1] and Doughty et al. [5]. However, while these early studies correctly identified important features of the system, they had to rely on rough estimates for several key reactions. In developing the present mechanism we have been able to draw on a number of recent experimental or high-level theoretical studies, mostly prompted by the interest in C_2H_4 oxidation in the troposphere [30, 38]. Furthermore, we conducted a theoretical study of $C_2H_3 + O_2$, as discussed below.

The reactions of C_2H_4 with O_2 and HO_2 are expected to be important for initiation. There are no measurements of the $C_2H_4 + O_2$ reaction. Benson [39] proposed low-barrier (39 kcal/mol) pathways to vinoxy radicals and formaldehyde; these estimates were adopted in our previous work [19]. However, a recent theoretical study [40] indicate barriers of 60 kcal/mol or more for all product channels. In the present study, we have only included the abstraction channel (R10), but formation of c-C_2H_4O+O, $CH_2CHOO+H$, and CH_2CH_2OO should be considered at higher temperatures [40]. Here, the

reaction numbering refers to the listing in Table 2. The reaction of C_2H_4 with HO_2 is expected to lead to oxyrane, either directly (R9) or through a sequence involving the 2-hydroperoxyethyl radical (R39b, R40) [36]. The activation energy for the $C_2H_4 + HO_2$ reaction has been in discussion [1,27], but recent theoretical work [41] confirms that even the association channel has a fairly high barrier. Still, the reaction is important at high pressure and an accurate determination of the rate constant and branching fraction is desirable. Due to the low barrier of dissociation for CH_2CH_2OOH, the reaction with O_2 is not expected to be significant under the current conditions. A subset for oxyrane ($c-C_2H_4O$) and the oxyranyl radical ($c-C_2H_3O$) were drawn from literature [31,35].

After initiation, the key step under the investigated conditions is the reaction of C_2H_4 with OH. Experimental data for the overall reaction over a wide temperature range [27] indicate non-Arrhenius behavior and multiple product channels. The reaction is also important for consumption of C_2H_4 in the atmosphere; this has spawned experimental and theoretical work also at below ambient temperatures [42]. Recent theoretical studies [43,44] identify three important channels, CH_2CH_2OH (R8), $H+CH_2CHOH$ (ethenol) (R7), and $C_2H_3+H_2O$ (R4). The relative importance of the three channels is a complex function of pressure and temperature. At atmospheric pressure and temperatures <500 K, the reaction almost exclusively proceeds via (R8) to form CH_2CH_2OH with a slight negative temperature dependence [45–47]. At temperatures roughly between 800 and 1000 K, both bimolecular channels, (R7) and (R4), become competitive. The rate constant governing the path to $C_2H_3+H_2O$ shows a strong positive temperature dependence, which makes (R4) the predominant reaction channel above 1000 K. The addition channel (R8) has mostly drawn attention due to its role in atmospheric chem-

istry [30,38], but results have been reported also at higher pressures and temperatures of up to 800 K [48]. Recently, Senosiain et al. [44] did a thorough master equation study of the C_2H_4+OH reaction. Their results are supported by a wide range of experimental data, including the recent high-temperature shock tube results from Srinivasan et al. [49]. We have obtained data for the relevant temperature and pressure range by interpolation between the rate coefficients for specific pressures from Senosaian et al. (see Table 2).

Under the conditions of the present work, with high pressure and temperatures of 600–900 K, the recombination reaction to form hydroxyethyl (R8) is the dominant channel for C_2H_4+OH. The CH_2CH_2OH radical may decompose thermally, react with the O/H radical pool, or with stable species such as O_2. The rates for reactions of unsaturated alcohols with a CH_2=CHROH structure are generally somewhat faster than those of the corresponding alkenes [30], indicating that the ROH substituent activates the C=C bond [30,50,51]. However, the difference in rates are roughly within a factor of two at 298 K. By analogy with oxidation of C_2H_5 under similar conditions [19], we would expect the reaction with O_2 to be the major consumption step for CH_2CH_2OH. The reaction has a number of accessible product channels, including stabilization of $HOCH_2CH_2OO$, hydroxyoxirane + OH, vinyl alcohol + HO_2, and two formaldehyde + OH [52]. In the present work we have included only two of these channels,

$$CH_2CH_2OH + O_2 \rightleftharpoons CH_2CHOH + HO_2 \qquad (R25)$$

$$CH_2CH_2OH + O_2(+M) \rightleftharpoons HOCH_2CH_2OO(+M) \qquad (R26)$$

with rate constants estimated by analogy to C_2H_5+O_2. These values are in reasonable agreement with the single room-temperature, low pressure measurement for CH_2CH_2OH+O_2 [53], but a factor of five below the high-

pressure limit estimated by Zador et al. [52]. The fast reaction of CH_2CH_2OH with OH leads to addition to form the diol $HOCH_2CH_2OH$ (R22) [30]. This and other reactions of CH_2CH_2OH with the O/H radical pool cannot compete with the O_2 reaction under lean conditions but may gain importance under fuel-rich conditions. Another consumption channel that could become important under oxygen-deficient conditions is the isomerization to ethoxy,

$$CH_2CH_2OH \rightleftharpoons C_2H_5O \qquad \text{(R18b)}$$

We have drawn the rate constant for this step from the recent ab initio study of the reverse reaction by Zhang et al. [29].

Rate constants for the CH_2CHOH subset were estimated by analogy to reactions of C_2H_4 and C_2H_5OH. The $HOCH_2CH_2OO$ radical, once formed, may undergo thermal dissociation, as proposed by Waddington and coworkers [54, 55], or reaction. Recent theoretical work [25, 37] indicate that the thermal dissociation,

$$HOCH_2CH_2OO \rightleftharpoons CH_2O + CH_2O + OH \qquad \text{(R41)}$$

which involves a 1,5 hydrogen shift, is indeed quite fast and presumably the main consumption channel. By analogy with other peroxide radicals, $HOCH_2CH_2OO$ may also react by either abstracting an H atom from HO_2 (R42) or CH_2O (R43), or by delivering an oxygen atom to C_2H_4 (R44). Under the present conditions the $HOCH_2CH_2OOH$ adduct would be expected to dissociate to form an alkoxy radical, $HOCH_2CH_2O$, and OH. Also the diol formed by (R22) yields $HOCH_2CH_2O$ by a rapid reaction with OH [30]. The alkoxy radical may, similarly to tropospheric chemistry [30,38], dissociate by C–C bond fission $HOCH_2CH_2O(+M) \rightleftharpoons CH_2O+CH_2OH(+M)$ or react with O_2, $HOCH_2CH_2O+O_2 \rightleftharpoons HOCH_2CHO+HO_2$. The thermal dissociation has

8

an estimated barrier of 10 kcal/mol [56–58], somewhat higher than for other β-hydroxy alkoxy radicals. It has been measured to be 1.3×10^5 s^{-1} at 298 K and 1 atm, about a factor of four below the estimated high-pressure limit at this temperature [58]. The reaction with O_2 can be expected to proceed with a rate constant of roughly k(RCH_2O+O_2) = 3.6×10^{10}exp(-550/T) cm^3 mol^{-1} s^{-1} [59]. In the troposphere, these two reactions compete [56, 60–62], but at the higher pressures and temperatures of the present study, thermal dissociation dominates, and we assume it to occur instantaneously in the mechanism.

Despite recent progress [6, 24, 63–65], details of the C_2H_3 + O_2 reaction are still in question and reliable rate constants over a wider range of pressure and temperature are not available. Initially density functional theory geometries (B3LYP/6-311G(d,p)) taken from the literature [64, 66] were used in the CBS-QB3 composite approach [67] to derive the potential energy diagram (PED) shown in Fig. 1. The stable intermediates and reaction pathways are mostly taken from the dominant channels identified in the work of Mebel et al. [64] on C_2H_3 + O_2. These are formation of collisionally stabilized C_2H_3OO, C_2H_2 + HO_2, C_2H_3O + O and isomerization to the dioxyranyl-methyl radical which can then further dissociate. Formation of CH_2O + HCO along with a minor path to CH_3 + CO_2 has been considered previously; here we add a new path to CH_3O + CO based on the work of Wang et al. [66]. This preliminary PED was analyzed via RRKM theory as implemented in the MultiWell program [68, 69], and detailed in the Supplemental Material, which showed that the branching ratio for products arising from dioxyranylmethyl decomposition was essentially independent of temperature and pressure, and was about 95% CH_2O + HCO with about 4% CH_3O + CO and less than 1% CH_3 + CO_2. Next, critical energies were refined at

higher levels of ab initio theory. Geometries and frequencies (scaled by a standard factor of 0.954) were computed at the QCISD/6-311G(d,p) level of theory, and these results are detailed in the Supplemental Material (Tables S1 and S2). The energies indicated on Fig. 1 were then obtained by extrapolation of coupled cluster (CCSD(T)) results, based on spin restricted open-shell wavefunctions with the aug-cc-pVTZ and aug-cc-pVQZ basis sets, to the complete basis set limit. Corrections were made for core-valence electron correlation and scalar relativistic effects (Supplemental Material, Table S3). These more sophisticated calculations largely confirm the CBS-QB3 data, to within around 1 kcal mol^{-1}, with the exception of the barrier for dioxiranylmethyl dissociation (TS3) which was lowered by ca. 4 kcal mol^{-1}.

Rate constants over 0.003 - 100 bar of N_2 at 300 - 2000 K were obtained via RRKM analysis and are summarized in the Supplemental Material. The channel to CH_2O+HCO (R12), generally the dominant product channel in combustion [6], is under the present conditions secondary to stabilization of the peroxy radical CH_2CHOO. Little has been reported about the reactivity of CH_2CHOO, so in the present work rate constants have been estimated by analogy to other peroxides. Its enthalpy of formation (Table 1) was assessed via the computed CCSD(T) enthalpy change for the isodesmic process $C_2H_3OO + CH_4 \rightarrow CH_3OO + C_2H_4$, coupled with experimental data for the other three species. Similarly, the thermochemistry of C_2H_3OOH was derived via consideration of $C_2H_3OOH + HO_2 \rightarrow C_2H_3OO + H_2O_2$. Thermochemical corrections for hindered internal rotation were taken from the literature [70].

Results and Discussion

Mixtures of C_2H_4 (about 1000 ppm) and O_2 highly diluted in N_2 were reacted at a pressure of 60 bar and stoichiometric ratios representing reducing, stoichiometric, and oxidizing conditions. The flow rate of 3 L min^{-1} (STP) resulted in (temperature dependent) residence times of 10-15 s in the isothermal zone of the reactor. The diluted conditions ensured a low heat release during the reaction and calculations of the adiabatic temperature rise gave values <26 K for all experiments. The carbon balances closed within 10%. From an estimate of the H_2O concentration, similar values were found for H and O. The experimental data were obtained as mole fractions as a function of the reactor temperature from 600–900 K using intervals of 25 K. The lower bound of the temperature interval (600 K) was well below the temperature where reactant conversion initiated.

Figure 2 compares experimental and modeling results at reducing conditions, whereas data sets obtained at stoichiometric and oxidizing conditions are presented in Figs. 3 and 4, respectively. The numerical predictions of the concentration profiles were obtained from plug flow simulations using the SENKIN code [71] from the CHEMKIN–II library [72].

The modeling predictions are generally in good agreement with the experimental results, even though the temperature for onset of reaction (725–750 K) is slightly underpredicted. Under reducing and stoichiometric conditions (Figs. 2 and 3), C_2H_4 was converted mainly to CO and to a lesser extent CO_2, while under oxidizing conditions (Fig. 4) CO and CO_2 were observed in comparable quantities above 750 K. Under reducing conditions, also minor amounts of C_2H_6 and CH_4 were detected. It is likely that c-C_2H_4O

11

and CH_2CHOH are formed in similar concentrations ($\sim$50 ppm), but these components were not quantified in the analysis.

Figure 5 provides an overview of the most important oxidation pathways for C_2H_4, according to the model. Upon initiation, the oxidation pathway depends on the composition of the O/H radical pool. Under lean conditions C_2H_4 reacts mainly with OH to form CH_2CH_2OH (R8) and, to a lesser degree, C_2H_3 (R4). Hydroxyethyl may recombine with O_2 to form hydroxyethyl peroxide (R26), which rapidly dissociates to CH_2O and OH (R40), or it may react with O_2 (R25) to form CH_2CHOH. The dominating sequence (R8), (R26), (R40) corresponds to the mechanism proposed by Waddington and coworkers for low temperature oxidation of alkenes [54, 55]. Overall this sequence is chain-propagating ($C_2H_4+O_2 \rightarrow 2CH_2O$). A secondary oxidation is initiated through $C_2H_4 + HO_2$ leading to CH_2CH_2OH (R39b), which dissociates to oxirane + OH (R40). Oxyranyl reacts with OH or HO_2 (R31, R32) to form the oxyranyl radical, which subsequently decomposes thermally (R35, R36).

Under stoichiometric and reducing conditions the oxygen availability is decreased and atomic hydrogen becomes more important as a chain carrier. Recombination of C_2H_4 with H to form C_2H_5 is here an important consumption step. Ethyl is partly recycled to C_2H_4 through reaction with O_2, and partly converted to C_1 species through C_2H_5O. Due to the low O_2 concentration, dissociation of hydroxyethyl to CH_2CHOH (R17) or back to C_2H_4+OH (R8b) becomes more important. The isomerization to C_2H_5O (R18b) is negligible due to a high barrier. The oxidation pathway through C_2H_3 is also more active than under lean conditions. It involves formation of vinyl peroxy (R11), which according to the model isomerizes to a cyclic species before

dissociating to CH_2O and HCO. In this way the overall reaction is similar to (R12) that dominates at lower pressure and higher temperature.

A sensitivity analysis shows that the overall behavior of the model is not strongly affected by changes in rate constants within their estimated uncertainty. The oxidation pathways through C_2H_3 (R4, R11, R37, R38) and CH_2CH_2OOH (R39b, R40, R31, R35) serve to promote initiation, shifting it 25–50 K to lower temperatures. The pathway through CH_2CH_2OO (R26, R41) inhibits initiation, but at higher temperatures it promotes reaction and shifts the location of the CO peak 25 K to lower temperatures. The C_2H_4/C_2H_5 interconversion is important for the partitioning of CH_4, C_2H_6 and oxygenated intermediates under reducing conditions. However, quantification of c-C_2H_4O and CH_2CHOH formation under these conditions would be valuable to put additional constraints on the kinetic model.

Conclusions

A detailed chemical kinetic model for oxidation of C_2H_4 in the intermediate temperature range and high pressure was developed and validated experimentally. The reaction between C_2H_3 and O_2 was studied theoretically to obtain rate coefficients under high pressure conditions. The experiments, involving C_2H_4/O_2 mixtures diluted in N_2, were carried out in a high pressure flow reactor at 600–900 K and 60 bar, varying the reaction stoichiometry from very lean to fuel-rich conditions. Model predictions were satisfactory, except under very lean conditions. The governing reaction mechanisms were outlined based on calculations with the kinetic model. Under the investigated conditions the oxidation pathways for C_2H_4 are more complex than those prevail-

13

ing at higher temperatures and lower pressures. The major differences are the importance of the hydroxyethyl (CH_2CH_2OH) and 2-hydroperoxyethyl (CH_2CH_2OOH) radicals, formed from addition of OH and HO_2 to C_2H_4, and vinyl peroxide, formed from $C_2H_3 + O_2$. Hydroxyethyl is oxidized through the peroxide $HOCH_2CH_2OO$ (lean conditions) or through ethenol (low O_2 concentration), while 2-hydroperoxyethyl is converted through oxirane.

Acknowledgments

References

[1] Wilk, R. D., Pitz, W. J., Westbrook, C. K., Cernansky, N. P. Proc. Combust. Inst. 23 (1990) 203-210.

[2] Dagaut, P., Boettner, J. C., Cathonnet, M. Int. J. Chem. Kinet. 22 (1990) 641.

[3] Vaughn, C. B., Sun, W. H., Howard, J. B., Longwell, J. P. Combust. Flame 84 (1991) 38-46.

[4] Marinov, N., Malte, P. C. Int. J. Chem. Kinet. 27 (1995) 957-986.

[5] Doughty, A., Barnes, F. J., Bromly, J. H., Haynes, B. S. Proc. Combust. Inst. 26 (1996) 589-596.

[6] Carriere, T., Westmoreland, P. R., Kazakov, A., Stein, Y. S., Dryer, F. L. Proc. Combust. Inst. 29 (2002) 1257–1266.

[7] Jallais, S., Bonneau, L., Auzanneau, M., Naudet, V., Bockel-Macal, S. Ind. Eng. Chem. Res. 41 (2002) 5659-5667.

[8] Homer, J. B., Kistiakowsky, G. B. J. Chem. Phys. 47 (1967) 5290.

[9] Baker, J. A., Skinner, G. B. Combust. Flame 19 (1972) 347-350.

[10] Hidaka, Y., Kataoka, T., Suga, M. Bull. Chem. Soc. Jpn. 47 (1974) 2166-2170.

[11] Jachimowski, C. J. Combust. Flame 29 (1977) 55-66.

[12] Hidaka, Y., Nishimori, T., Sato, K., Henmi, Y., Okuda, R., Inami, K., Higashihara, T. Combust. Flame 117 (1999) 755-776.

[13] Egolfopoulos, F. N., Zhu, D. L., Law, C. K. Proc. Combust. Inst. 23 (1990) 471-478.

[14] Bernstein, J. S., Fein, A., Choi, J. B., Cool, T. A., Sausa, R. C., Howard, S. L., Locke, R. J., Miziolek, A. W. Combust. Flame 92 (1993) 85.

[15] Wang, H., Frenklach, M. Combust. Flame 110 (1997) 173–221.

[16] Bhargava, A., Westmoreland, P. R. Combust. Flame 113 (1998) 333–347.

[17] Bhargava, A., Westmoreland, P. R. Combust. Flame 115 (1998) 456–467.

[18] Rasmussen, C. L., Hansen, J., Marshall, P., Glarborg, P. Int. J. Chem. Kinet., in press.

[19] Rasmussen, C. L., Jacobsen, J.G., Glarborg, P. Int. J. Chem. Kinet., in press.

[20] Ing, W.-C., Sheng, C. Y., Bozzelli, J. W. Fuel Proc. Tech. 83 (2003) 111–145.

[21] Yamada, T., Bozzelli, J. W., Lay, T. J. Phys. Chem. A 103 (1999) 7646-7655.

[22] Burcat, A., Ruscic, B. "*Third Millennium Ideal Gas and Condensed Phase Thermochemical Database for Combustion with Updates from Active Thermochemical Tables*", Report TAE960, Technion Israel Inst. of Technology, 16th September 2005.

[23] da Silva, G., Kim, C.-H., Bozzelli, J. W. J. Phys. Chem. A 110 (2006) 7925-7934.

[24] Chang, A. Y., Bozzelli, J. W., Dean, A. M. Z. Phys. Chem. 214 (2000) 1533-1568.

[25] Olivella, S., Sole, A. J. Phys. Chem. A 108 (2004) 11651-11663.

[26] Senosiain, J. P., Klippenstein, S. J., Miller, J. A. J. Phys. Chem. A 110 (2006) 5772–5781.

[27] Baulch, D. L., Bowman, C. T., Cobos, C. J., Cox, R. A., Just, T.; Kerr, J. A., Pilling, M. J., Stocker, D., Troe, J., Tsang, W.; Walker, R. W., Warnatz, J. J. Phys. Chem. Ref. Data 34 (2005) 757–1397.

[28] Hua, H., Ruscic, B., Wang, B. Chem. Phys. 311 (2005) 335–341.

[29] Zhang, Y., Zhang, S., Li, Q. S. Chem. Phys. 308 (2005) 109-116.

[30] Mellouki, A., LeBras, G., Sidebottom, H. Chem. Rev. 103 (2003) 5077–5096.

[31] Joshi, A., You, X., Barckholtz, T.A., Wang, H. J. Phys. Chem. A 109 (2005) 8016–8027.

[32] Lifshitz, A., Ben-Hamou, H. J. Phys. Chem. 87 (1983) 1782.

[33] Bogan, D.J., Hand, C.W. J. Phys. Chem. 82 (1978) 2067.

[34] Baldwin, R.R., Keen, A., Walker, R.W. J. Chem. Soc. Faraday Trans. 80 (1984) 435.

[35] Dagaut, P., Voisin, D., Cathonnet, M., McGuinness, M., Simmie, J. M. Combust. Flame 106 (1996) 62-68.

[36] Bozzelli, J. W., Sheng, C. J. Phys. Chem. A 106 (2002) 1113-1121.

15

[37] Kuwata, K. T., Dibble, T. S., Sliz, E., Petersen, E. B. J. Phys. Chem. A 111 (2007) 5032-5042.

[38] Orlando, J. J., Tyndall, G. S., Wallington, T. J. Chem. Rev. 103 (2003) 4657–4689.

[39] S. W. Benson. Int. J. Chem. Kinet. 28 (1996) 665–672.

[40] Hua, H., Ruscic, B., Wang, B. Chem. Phys. 311 (2005) 335–341.

[41] Rienstra-Kiracofe, J.C., Allen, W.D., Schaefer III, H.F. J. Phys. Chem. A 104 (2000) 9823-9840

[42] Cleary, P. A., Romero, M. T. B., Blitz, M. A., Heard, D. E., Pilling, M. J., Seakins, P. W., Wang, L. Phys. Chem. Chem. Phys. 8 (2006) 5633-5642.

[43] Zhu, R. S., Park, J., Lin, M. C. Chem. Phys. Lett. 408 (2005) 25–30.

[44] Senosiain, J. P., Klippenstein, S. J., Miller, J. A. J. Phys. Chem. A 110 (2007) 6960–6970.

[45] Atkinson, R., Perry, R. A., Pitts, Jr., J. N. J. Chem. Phys. 66 (1977) 1197–1201.

[46] Liu, A., Mulac, W. A., Jonah, C. D. J. Chem. Phys. 92 (1988) 3828–3833.

[47] Diau, E. W.-G., Lee, Y.-P. J. Chem. Phys. 96 (1992) 377.

[48] Homer, J. B., Kistiakowsky, G. B. J. Chem. Phys. 47 (1967) 5290.

[49] Srinivasan, N. K., Su, M.-C., Michael, J. V. Phys. Chem. Chem. Phys. 9 (2007) 4155-4163.

[50] Papagni, C., Arey, J., Atkinson, R. Int. J. Chem. Kinet. 33 (2001) 142-147.

[51] Orlando, J. J., Tyndall, G. S., Ceazan, N. J. Phys. Chem. A 105 (2001) 3564-3569.

[52] Zador, J., Fernandes, R.X., Georgievskii, Y., Meloni, G., Taatjes, C.A., Miller, J.A. Proc. Combust. Inst. 32 (2009), submitted

[53] Miyoshi, A., Matsui, H., Washida, N. Chem. Phys. Lett. 160 (1989) 291-294.

[54] Ray, D. J. M., Diaz, R. R., Waddington, D. J. Proc. Combust. Inst. 14 (1973) 259.

[55] Ray, D. J. M., Waddington, D. J. Combust. Flame 20 (1973) 327.

[56] Orlando, J. J., Tyndall, G. S., Bilde, M., Ferronato, C. J., Wallington, T. J., Verecken, L., Peeters, J. J. Phys. Chem. A 102 (1998) 8116-8123.

[57] Vereecken, L., Peeters, J. J. Phys. Chem. A 103 (1999) 1768.

[58] Caralp, F., Forst, W., Rayez, M.-T. Phys. Chem. Chem. Phys. 5 (2003) 476-486.

[59] Calvert, J. G.; Atkinson, R.; Kerr, J.A.; Madronich, S., Yarwood, G., *The Mechanism of Atmospheric Oxidation of the Alkenes;* Oxford University Press, New York: 2000.

[60] Niki, H., Maker, P. D., Savage, C. M., Breitenbach, L. P. J. Phys. Chem. 82 (1978) 135-137.

[61] Niki, H., Maker, P. D., Savage, C. M., Breitenbach, L. P. Chem. Phys. Lett. 80 (1981) 499-503.

[62] Barnes, I., Becker, K. H., Ruppert, L. Chem. Phys. Lett. 203 (1993) 295-301.

[63] Carpenter, B. K. J. Phys. Chem. A 105 (2001) 4585.

[64] Mebel, A. M., Diau, E. W. G., Lin, M. C., Morokuma, K. J. Am. Chem. Soc. 118 (1996) 9759–9771.

[65] Mebel, A. M., Kislov, V. V. J. Phys. Chem. A 109 (2005) 6993-6997.

16

[66] Wang, B., Hou, H., Gu, Y. J. Phys. Chem. A 103 (1999) 8021-8029.

[67] Montgomery Jr., J.A., Frisch, M.J., Ochterski, J.W., Petersson, G.A. J. Chem. Phys. 110 (1999) 2822-2827

[68] Barker, J.R., Ortiz, N.F., Preses, J.M., Lohr, L.L., Maranzana, A., Stimac, P.J. MultiWell-2.08 program (University of Michigan, Ann Arbor, MI, 2008).

[69] Barker, J.R. Int. J. Chem. Kinet. 33 (2001) 232-245.

[70] Sebbar, N., Bockhorn, H., Bozzelli, J.W. Phys. Chem. Chem. Phys. 4 (2002) 3691.

[71] Lutz, A. E., Kee, R. J., Miller, J. A. *"Senkin: A Fortran Program for Predicting Homogeneous Gas Phase Chemical Kinetics With Sensitivity Analysis"*, Sandia Report SAND87–8248·UC–401, Sandia National Laboratories, Livermore, CA, 1990.

[72] Kee, R. J., Rupley, F. M., Miller, J. A. *"Chemkin II: A Fortran Chemical Kinetics Package for the Analysis of Gas Phase Chemical Kinetics"*, Sandia Report SAND89–8009B·UC–706, Sandia National Laboratories, Livermore, CA, 1989.

17

Species	H_{298}	S_{298}	$C_{p,300}$	$C_{p,400}$	$C_{p,500}$	$C_{p,600}$	$C_{p,800}$	$C_{p,1000}$	$C_{p,1500}$	Ref.
CH_2CHOO	25.65	69.34	16.50	19.58	22.09	24.14	27.15	29.18	32.37	pw
CH_2CHOOH	-8.80	64.37	18.67	21.81	24.47	26.70	30.14	32.55	36.12	pw
CH_2CH_2OOH	11.22	81.89	20.28	23.56	26.33	28.68	32.38	35.12	39.65	[20]
CH_2CH_2OH	-5.70	69.70	16.47	19.38	22.06	24.40	27.94	30.70	35.00	[21, 22]
CH_2CHOH	-30.00	61.73	14.83	18.16	20.75	22.74	25.61	27.70	31.14	[23]
c-$C_2H_3O_2$	41.61	67.33	14.10	17.92	21.16	23.88	28.03	30.81	34.19	[24]
$HOCH_2CH_2OO$	-40.30	78.01	20.77	25.30	29.39	32.83	38.06	41.81	47.53	[25],a

a: entropy and heat capacity were drawn from Da Silva, Liang, Bozzelli and Farrell, unpublished work (2007).

Table 1: Thermodynamic properties of selected species in the reaction mechanism. Units are kcal mol^{-1} for H, and cal mol^{-1} K^{-1} for S and C_p. Temperature (T) range is in K.

		A [cm,mole,s]	β	E_a [cal/mole]	Source
1.	$C_2H_4 + H \rightleftharpoons C_2H_3 + H_2$	2.4E02	3.620	11266	[19]
2.	$C_2H_4 + O \rightleftharpoons CH_3 + HCO$	3.9E12	0.000	1494	[19], a
		6.2E13	0.000	6855	
3.	$C_2H_4 + O \rightleftharpoons CH_2CHO + H$	1.7E12	0.000	1494	[19], a
		2.8E13	0.000	6855	
4.	$C_2H_4 + OH \rightleftharpoons C_2H_3 + H_2O$	1.3E-1	4.200	−860	[26]
5.	$C_2H_4 + OH \rightleftharpoons CH_3 + CH_2O$	3.3E11	0.000	9079	[26], b
6.	$C_2H_4 + OH \rightleftharpoons CH_3CHO + H$	1.4E33	−6.114	24907	[26], b
7.	$C_2H_4 + OH \rightleftharpoons CH_2CHOH + H$	1.7E13	0.000	11527	[26], b
8.	$C_2H_4 + OH \rightleftharpoons CH_2CH_2OH$	2.4E20	−2.399	3294	[26], b
9.	$C_2H_4 + HO_2 \rightleftharpoons c\text{-}C_2H_4O + OH$	2.2E12	0.000	17200	[27]
10.	$C_2H_4 + O_2 \rightleftharpoons C_2H_3 + HO_2$	7.1E13	0.000	60010	[28]
11.	$C_2H_3 + O_2 \rightleftharpoons CH_2CHOO$	1.1E12	0.000	−1680	pw, c
12.	$C_2H_3 + O_2 \rightleftharpoons CH_2O + HCO$	6.3E12	0.000	3130	pw, c
13.	$C_2H_3 + O_2 \rightleftharpoons CH_2CHO + O$	4.8E12	0.000	4800	pw, c
14.	$C_2H_3 + O_2 \rightleftharpoons C_2H_2 + HO_2$	7.6E11	0.000	7930	pw, c
15.	$C_2H_3 + O_2 \rightleftharpoons CH_3O + CO$	2.8E11	0.000	3130	pw, c
16.	$C_2H_3 + O_2 \rightleftharpoons CH_3 + CO_2$	1.3E10	0.000	3130	pw, c
17.	$CH_2CH_2OH \rightleftharpoons CH_2CHOH + H$	2.2E05	2.840	32920	[21], k_∞
18.	$C_2H_5O \rightleftharpoons CH_2CH_2OH$	2.8E-29	11.900	4450	[29], k_∞
19.	$CH_2CH_2OH + H \rightleftharpoons CH_3 + CH_2OH$	1.0E14	0.000	0	$k_{C_2H_5+H}$
20.	$CH_2CH_2OH + O \rightleftharpoons CH_2O + CH_2OH$	4.0E13	0.000	0	$k_{C_2H_5+O}$
21.	$CH_2CH_2OH + OH \rightleftharpoons CH_2CHOH + H_2O$	2.4E13	0.000	0	$k_{C_2H_5+OH}$
22.	$CH_2CH_2OH + OH \rightleftharpoons HOCH_2CHOH$	3.3E13	0.000	0	[30], 298 K
23.	$CH_2CH_2OH + HO_2 \rightleftharpoons C_2H_5OH + O_2$	1.0E12	0.000	0	$k_{C_2H_5+HO_2}$
24.	$CH_2CH_2OH + HO_2 \rightarrow HOCH_2CH_2O + OH^d$	3.0E13	0.000	0	$k_{C_2H_5+HO_2}$
25.	$CH_2CH_2OH + O_2 \rightleftharpoons CH_2CHOH + HO_2$	1.4E07	1.090	−1975	$k_{C_2H_5+O_2}$
26.	$CH_2CH_2OH + O_2(+M) \rightleftharpoons HOCH_2CH_2OO(+M)$	2.0E10	0.980	−64	$k_{C_2H_5+O_2}$
	Low pressure limit:	8.5E29	−4.290	220	
	Troe parameters: 0.897 1.E-30 601 1.E30				
27.	$c\text{-}C_2H_4O + H \rightleftharpoons CH_3CHO + H$	5.6E13	0.000	10950	[31]
28.	$c\text{-}C_2H_4O + H \rightleftharpoons c\text{-}C_2H_3O + H_2$	2.0E13	0.000	8310	[32]
29.	$c\text{-}C_2H_4O + H \rightleftharpoons C_2H_4 + OH$	9.5E10	0.000	5000	[32]
30.	$c\text{-}C_2H_4O + O \rightleftharpoons c\text{-}C_2H_3O + OH$	1.9E12	0.000	5250	[33]
31.	$c\text{-}C_2H_4O + OH \rightleftharpoons c\text{-}C_2H_3O + H_2O$	1.8E13	0.000	3610	[34]
32.	$c\text{-}C_2H_4O + HO_2 \rightleftharpoons c\text{-}C_2H_3O + H_2O_2$	4.0E12	0.000	17000	[35]
33.	$c\text{-}C_2H_4O + O_2 \rightleftharpoons c\text{-}C_2H_3O + HO_2$	4.0E13	0.000	61500	[35]
34.	$c\text{-}C_2H_3O \rightleftharpoons CH_2CHO$	8.7E31	−6.900	14994	[31], k_∞
35.	$c\text{-}C_2H_3O \rightleftharpoons CH_2CO + H$	5.0E13	0.000	14863	[31], k_∞
36.	$c\text{-}C_2H_3O \rightleftharpoons CH_3 + CO$	7.1E12	0.000	14280	[31], k_∞
37.	$CH_2CHOO \rightleftharpoons c\text{-}C_2H_3O_2$	3.9E09	0.000	22250	[20], b
38.	$c\text{-}C_2H_3O_2 \rightleftharpoons CH_2O + HCO$	6.1E10	0.000	914	[20], b
39.	$C_2H_2OOH \rightleftharpoons C_2H_4 + HO_2$	1.3E11	0.520	16150	[36], k_∞
40.	$C_2H_2OOH \rightleftharpoons c\text{-}C_2H_4O + OH$	1.3E10	0.720	15380	[36], k_∞
41.	$HOCH_2CH_2OO \rightarrow CH_2O + CH_2O + OH$	9.4E08	0.994	22250	[37], k_∞
42.	$HOCH_2CH_2OO + HO_2 \rightarrow HOCH_2CH_2OOH + O_2^{d,e}$	1.0E12	0.000	−1100	$k_{CH_3OO+HO_2}$
43.	$HOCH_2CH_2OO + CH_2O \rightarrow HOCH_2CH_2OOH + HCO^{d,e}$	4.1E04	2.500	10206	$k_{HO_2+CH_2O}$
44.	$HOCH_2CH_2OO + C_2H_4 \rightarrow HOCH_2CH_2O + c\text{-}C_2H_4O^d$	2.2E12	0.000	17200	$k_{HO_2+C_2H_4}$
45.	$HOCH_2CH_2OH + OH \rightarrow HOCH_2CH_2O + H_2O^d$	9.0E12	0.000	0	[30]

a: Duplicate reaction; b: Interpolation for 60 bar and 600–900 K; c: The values apply for 60 bar and 500–900 K. The atmospheric pressure rate constants (200–3000 K) are $k_{11} = 1.1 \times 10^{36}$ $T^{-8.58}$ exp(-2290/RT), $k_{12} = 4.0 \times 10^{15}$ $T^{-0.959}$ exp(-580/RT), $k_{13} = 2.0 \times 10^9$ $T^{0.923}$ exp(-226/RT), $k_{14} = 4.4 \times 10^1$ $T^{2.95}$ exp(-186/RT), $k_{15} = 1.9 \times 10^{14}$ $T^{-0.959}$ exp(-580/RT), and $k_{16} = 2.1 \times 10^{13}$ $T^{-0.959}$ exp(-580/RT); d: The product $HOCH_2CH_2O$ is assumed to dissociate immediately to CH_2OH+CH_2O; e: The product $HOCH_2CH_2OOH$ is assumed to dissociate immediately to $HOCH_2CH_2O+OH$.

Table 2: Selected reactions from the C_2 hydrocarbon subset. Parameters for use in the modified Arrhenius expression $k = AT^\beta \exp(-E/[RT])$. Units are mol, cm, s, cal.
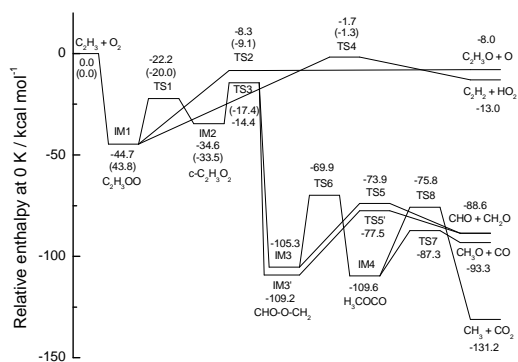
Figure 1: Relative enthalpies of minima and transition states for the C_2H_3 + O_2 reaction computed at the CBS-QB3 level of theory. CCSD(T) results extrapolated to the complete basis set limit are shown in parentheses.
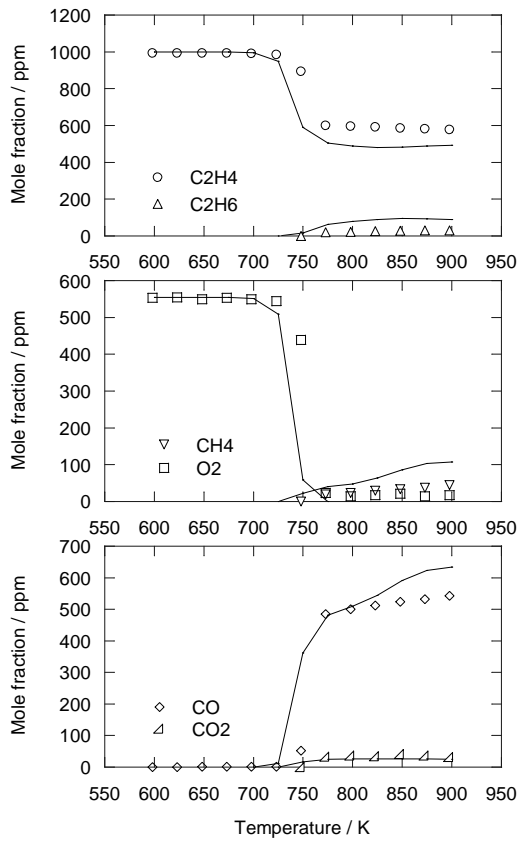
Figure 2: Comparison of experimental and predicted concentration profiles as a function of the reactor temperature for the reducing experiment with C_2H_4/O_2 ($\lambda = 0.2$). The pressure was 60 bar and the reactor residence time was 8892/T (s·K). The inlet composition was 1000 ppm C_2H_4, 555 ppm O_2, and N_2 by difference. The symbols mark experimental data while solid lines denote model predictions obtained at isothermal conditions.
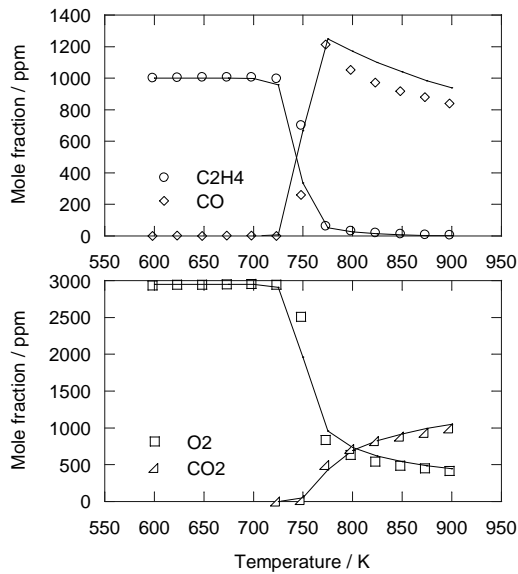
Figure 3: Comparison of experimental and predicted concentration profiles as a function of the reactor temperature for the stoichiometric experiment with C_2H_4/O_2 ($\lambda = 0.981$). The pressure was 60 bar and the reactor residence time was 8760/T (s·K). The inlet composition was 1000 ppm C_2H_4, 2950 ppm O_2, and N_2 by difference. The symbols mark experimental data while solid lines denote model predictions obtained at isothermal conditions.
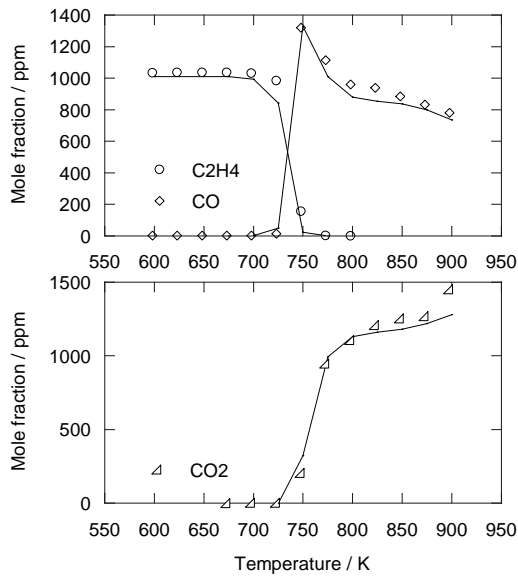
Figure 4: Comparison of experimental and predicted concentration profiles as a function of the reactor temperature for the oxidizing experiment with C_2H_4/O_2 ($\lambda = 19.8$). The pressure was 60 bar and the reactor residence time was $8804/T$ (s·K). The inlet composition was 1000 ppm C_2H_4, 6.0% O_2, and N_2 by difference. The symbols mark experimental data while solid lines denote model predictions obtained at isothermal conditions.
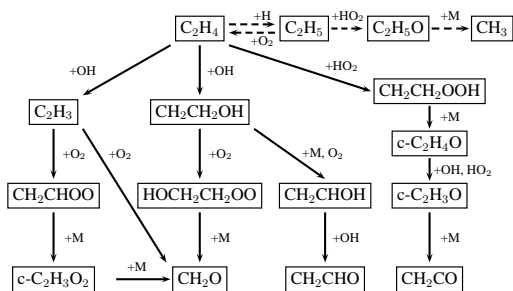
Figure 5: Main reaction pathways for C$_2$H$_4$ conversion at the investigated conditions. The solid lines denote pathways important over the range of stoichiometries investigated, while dashed lines denote pathways important only under reducing conditions.

SUPPLEMENTAL MATERIAL:

Vinylperoxy supplemental material

Chemical kinetic model